



SMA Newsletter



Number 3

Submillimeter Array Newsletter

21 December 2006

The Submillimeter Array (SMA) is a pioneering radio-interferometer dedicated to a broad range of astronomical studies including protostellar disks and outflows; evolved stars; the Galactic Center and AGN; normal and luminous galaxies; and the solar system. Located on Mauna Kea, Hawaii, the SMA is a collaboration between the Smithsonian Astrophysical Observatory and the Academia Sinica Institute of Astronomy and Astrophysics.

Contents

1 From the Director	1
2 Science Highlights	2
2.1 Galactic Center Legacy Program	2
2.1.1 Polarization and Spectrum of Sgr A*	2
2.1.2 Ionized Gas in the Central Parsec	3
2.1.3 Molecular Gas in the Circumnuclear Disk (CND)	3
2.2 SMA Constraints on the Structure of Circumstellar Disks	4
3 Engineering Highlights	6
4 Proposal Statistics (November 2006 - April 2007)	7
5 Recent SMA publications	9
6 Other news	13

1 From the Director

In a continued effort to optimize the SMA for scientific observations, particularly in the 300 GHz frequency band where it is most sensitive to emission from the cool universe, antenna 7 was removed from the array for much of the latter half of the year in order to bring it up to full specifications. As a result of concerted effort by engineering and technical staff, many of whom are required to maintain and operate the array, the upgrades to antenna 7 were completed in about half the time required to complete similar upgrades to antenna 8. During the same period, the antenna 7 cryostat was removed to enable upgrades to be made to its 200, 300 and 600 GHz receivers; and for instal-

lation of the 400 GHz unit which will improve array sensitivity in the overlap region (320 – 355 GHz) of the 300 and 400 GHz receiver bands. As the upgraded receiver set for antenna 7 is not expected to be ready for installation until early in the New Year, a spare 3-receiver set, taken from antenna 6 which was recently upgraded to include a 400 GHz unit, has been installed to enable eight-antenna operation for the first time since April. Fringes were obtained on all eight antennas just a few nights ago. Given that no more major refits are planned for the SMA antennas, and that installation of the additional 400 GHz receiver sets will be done sequentially, we expect to maintain an eight-element array for much of the coming year.

Ray Blundell

2 Science Highlights

2.1 Galactic Center Legacy Program

A coordinated effort was begun to study the Galactic Center region with the SMA in the spring and summer of 2005. The program consisted of eight projects supported by about 20 observational tracks with the Array. We describe the results of three of the projects to study SgrA* through its continuum emission, the ionized gas in the central cavity through the H30 α recombination line and the circumnuclear disk through emission in several molecular lines.

2.1.1 Polarization and Spectrum of Sgr A*

Observations of the continuum emission from Sgr A*, the radio source associated with the black hole in the center of our galaxy, at 230, 345 and 690 GHz have led to new insights into the nature of the source and the black hole accretion disk. The main results are: (1) the rotation measure has been definitively measured to be -5.6×10^5 rad m² and stable, which implies an accretion rate of about $10^{-8} M_{\odot}\text{yr}^{-1}$; (2), the intrinsic polarization varies substantially on timescales of less than an hour, which suggests that it may be possible to trace emission “events” arising in the orbiting gas within 10 Schwarzschild radii (r_s) of the black hole; and (3) the peak of the SED determined from simultaneous measurements at 230 and 690 GHz is about 350 GHz, lower than previously thought, which limits the luminosity to about $200 L_{\odot}$, or about $10^{-9} L_{Edd}$. Dan Marrone’s thesis was based on this work. It is the first Harvard PhD thesis devoted entirely to research done on the SMA.

Figure 2.1 shows a typical image of the linearly polarized continuum emission from SgrA* at 230 GHz. The source is unresolved, but interferometric measurements are essential to isolate the emission of SgrA* from that of the surrounding dust. We measured the polarization characteristics separately and simultaneously for the two sidebands offset by 10 GHz. We interpreted the change in polarization angle as being caused by the effect of a Faraday screen, which is presumably the accretion envelope surrounding the black hole. From these measurements we deduced the rotation measure (RM) and the intrinsic polarization angle of the emission. The daily averages of the rotation measure for six epochs at 230 GHz and 4 epochs at 345 GHz are shown in Figure 2.2. The RM data are consistent with a constant value $-5.6 \pm 0.7 \times 10^5$ rad m⁻², while the intrinsic polarization is variable with a dispersion of 30 degrees. The rotation measure is proportional to the integral of the product of the line-of-sight component of the magnetic field and the ionized gas density. With various modeling assumptions: equipartition of energy, a power law density profile with an inner cut-off where the flow becomes relativistic, and a smooth magnetic field without reversals,

the accretion rate can be inferred. The estimate is $10^{-8} M_{\odot}\text{yr}^{-1}$ with a hard lower limit of $10^{-9} M_{\odot}\text{yr}$.

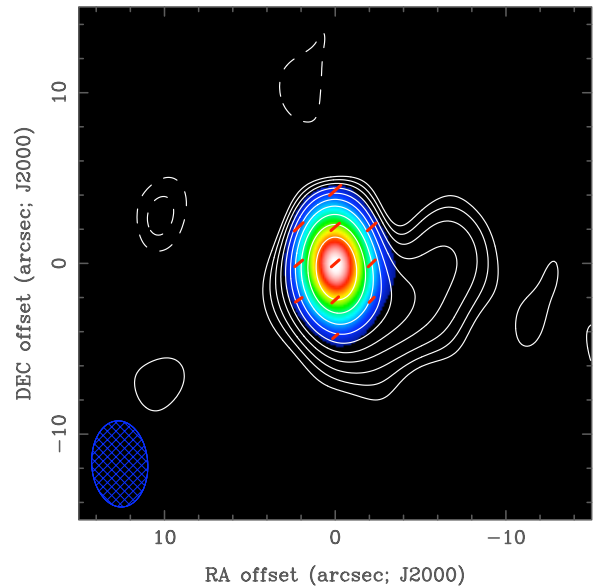


Figure 2.1: SMA image of Sgr A* at 230 GHz. The contours represent the total intensity and the color map traces the polarized flux. The vectors represent the polarization position angle at each point, their magnitude is proportional to the polarization fraction. Contours are spaced by factors of $\sqrt{2}$, starting at 3.5σ . The peak flux density was 3.8Jy.

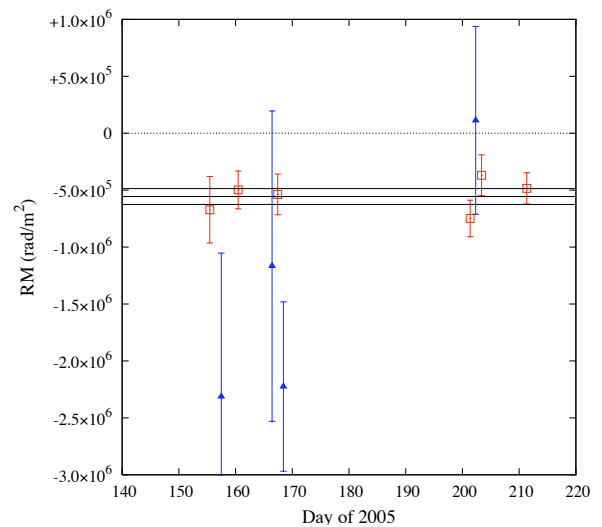


Figure 2.2: Measurements of the Faraday rotation measure (RM) in ten epochs from 2005. Measurements at 230 GHz (red) are approximately 4 times more sensitive to the RM than those at 345 GHz (blue) owing to the larger coverage in λ^2 at lower frequency. This is the first detection of Faraday rotation in Sgr A* through comparison of the simultaneous polarization measurements at two frequencies, which is immune to the effects of the large polarization variability in this source.

The behavior of the variable component of the linear polarization can best be seen in the plot of Stokes parameters shown in Figure 2.3. The variable polarization component appears to make two orbits around the point of ambient polarization. With this type of data it may be possible to follow a blob of synchrotron emitting gas as it spirals into the black hole from a radius of less than $10 r_s$. The temporal resolution available with the SMA should allow these events to be observed for any stable orbit (periods greater than 4 min).

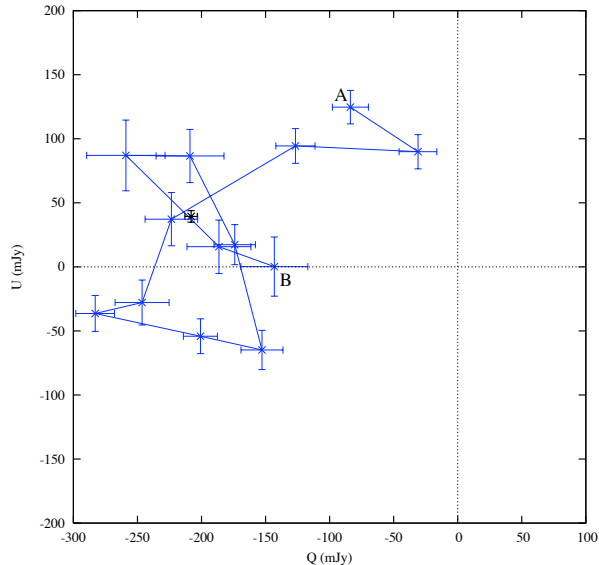


Figure 2.3: (Left) The time sequence of polarization measurements made on July 29, 2005 plotted in the Q-U Stokes parameter plane. The sequence begins at point A and the duration is about 3.5 hours. The track appears to orbit the mean polarization (black cross), as might be expected for a synchrotron hot spot orbiting the black hole.

In 2007 the SMA will continue observe Sgr A* in coordination with the VLT, Keck, Chandra, the CSO and other telescopes to try to catch more events like the one shown in Figure 2.1 and to characterize their emission processes.

2.1.2 Ionized Gas in the Central Parsec

The bandpass for the Sgr A* continuum measurements included the H30 α recombination line, so we were able to image this line with no additional tracks. Since only one pointing was done we only obtained the image in the central 53'' region (~ 2 pc) centered on Sgr A* with $5'' \times 3''$ angular resolution. The 2 GHz bandwidth of the SMA covered a velocity range of more than ± 1000 km/s. This line is an excellent tracer of the dense ionized streamers in the inner parsec. The intensity weighted velocity map is shown in Figure 2.4. The line is strongest near IRS13 and IRS2, suggesting that a significant amount of gas has been trapped

in the stellar cluster. The gas near IRS13 has two components separated by nearly 250 km/s which are not resolved spatially by the SMA (these components can be seen in the spectra). The large velocity gradient from NE of Sgr A* to SW suggests that a streamer of ionized gas is being accreted into the region close to Sgr A*. Higher resolution observations and detailed modeling efforts are underway in order to understand how the ionized streamer interacts with the stellar cluster in the vicinity of Sgr A*.

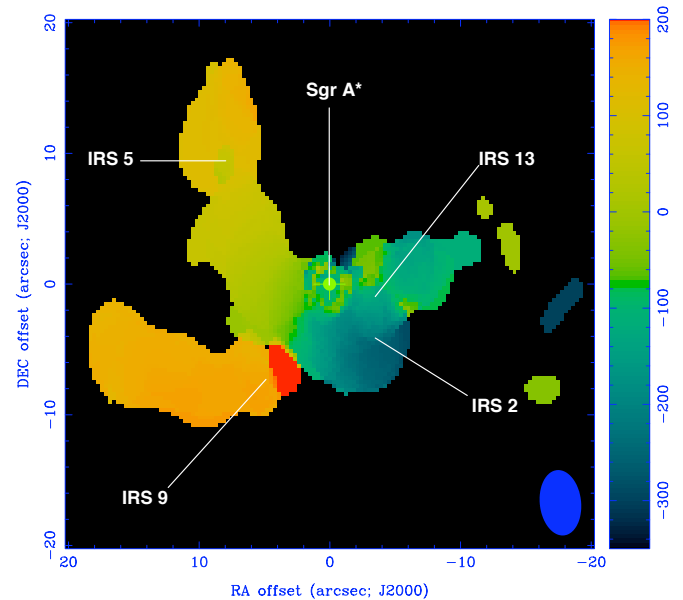


Figure 2.4: The intensity weighted velocity map shows the velocity field in the central parsec. The velocities are color coded from red (200 km/s) to blue (-350 km/s). The position of Sgr A* is marked by the small circle at the coordinate origin. Other well known infrared sources are also marked. The array beam is shown in the lower right.

2.1.3 Molecular Gas in the Circumnuclear Disk (CND)

We measured the distribution of four high-density tracers [HCN(4-3), CS(7-6), HCN(3-2) HCO⁺(3-2)] in the vicinity of Sgr A*. We produced mosaic images over 2 arcminutes around Sgr A*, encompassing the circumnuclear disk (CND). Using a 25-pointing mosaic (36'' primary beam) we have detected HCN(4-3) and CS(7-6) at 350 GHz, and with a 16-pointing mosaic (47'' primary beam) we have observed HCN(3-2) and HCO⁺(3-2) at 267 GHz. In Figure 5 we compare our HCN(4-3) results to the HCN(1-0) observations from OVRO (Christopher et al. 2005). All four lines of the lines we observed show their strongest emission in the southern part of the CND. The results indicate that the excitation is not uniform within the CND, i.e. the southern part is warmer and denser than the northern part.

The CND may not be a real disk, but an ensemble of different structures with different excitation levels. Emission is mostly located to the south, tracing the southwest lobe and the southern extension. CS is the highest-density tracer of our sample, and it is the only one completely absent from the northern part of the CND, which further strengthens the conclusion that the southern part is denser than the northern part.

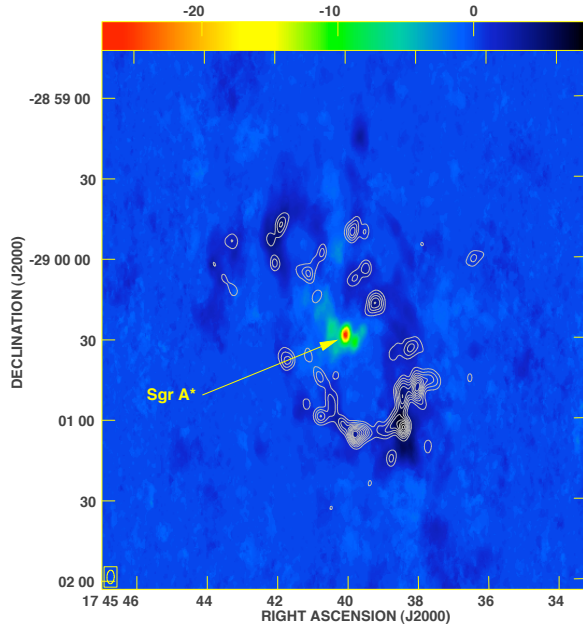


Figure 2.5: The distribution of HCN(4–3), shown in contours (the contour levels are in steps of 10% of the intensity peak, from 5×10^4 to 45×10^4 mJy/beam km/s). The color image (scale at the top) shows the HCN(1–0) emission in the CND and absorption in front of Sgr A* (from Christopher et al. 2005).

*Jim Moran for the SMA Galactic Center Team**

**The other SMA Galactic Center team members contributing to this report include Ray Blundell, Paul Ho, Dan Marrone, María Montero-Castaño, Sheng-Li Qin, Jun-Hui Zhao, Dennis Downes and Karl Schuster.*

References:

(1) Christopher, M. H., Scoville, N. Z., Stolovy, S. R., & Yun, Min S., 2005, ApJ, 622, 346

2.2 SMA Constraints on the Structure of Circumstellar Disks

With the growing number of planetary systems found around other stars, our attention is increasingly focused

on the origin of our Solar System and others like it. The key to addressing these issues is a better understanding of the process of planet formation. To learn about the mechanisms involved in creating planets and their efficiencies, we need to study the reservoirs of planet-building material, the disks around young stars. Because of their sensitivity to the amount and distribution of this raw material, high spatial resolution submillimeter observations provide direct views of the internal properties of circumstellar disks and therefore the initial conditions available for the planet formation process.

Using the SMA at 230 and 345 GHz, we have recently completed the largest interferometric survey of young disks to date, consisting of 24 objects in the nearby Tau-Aur and Oph-Sco star formation regions [1]. Figure 2.6 shows the aperture synthesis submillimeter continuum images of the survey disks. The aim of the survey is to characterize the structure and content of the molecular gas and dust phases in these disks. We have used the SMA continuum visibilities combined with the multiwavelength spectral energy distributions to measure disk structure parameters in the context of a simple model, including in particular the sizes and spatial density distributions. The typical disk in this sample has a radius of 200 AU and a density profile that drops off roughly inversely with radius ($\Sigma \propto r^{-1}$).

Submillimeter emission from disks is a diagnostic of the product of density and opacity. Therefore, constraints on the opacity are critical in comparing observations with the density requirements of planet formation models. The spectral shape of the submillimeter SED is related to the opacity (actually β where the opacity is $\kappa \propto \nu^\beta$), which is a probe of the dust grain size distribution and therefore the process of particle growth from ISM grains to planetesimals [3,4]. We have used the disk structure measurements from the SMA visibilities to correct the measured SED shapes for contamination from optically thick emission and determined the mean value of $\beta \approx 1.0$ for the sample. This low β value is consistent with maximum particle sizes of a few millimeters or more [5], indicating that dust grains have grown roughly four orders of magnitude since they were incorporated from the ISM.

These results are in good agreement with accretion disk models where the viscosity varies linearly with radius [2]. In the framework of a fiducial accretion disk model, we demonstrated that a turbulent viscosity parameter $\alpha \approx 0.01$ provides an excellent match to a wide range of observations including the median spatial density distribution, SED, and submillimeter surface brightness profile, along with the variations of disk sizes, fluxes, and mass accretion rates with stellar age. Figure 2.7 compares some of these evolutionary trends with accretion disk models. The value of α plays a critical role in setting the viscous evolution timescale for disks, and therefore the timeframe over which surface densities remain high enough for planets to form.

Future work with this survey will focus on interpreting the spatio-kinematics of the CO rotational line emission from these disks. These data can help to determine the vertical structure of the disk atmospheres [6], setting important constraints on gravitational sedimentation, irradiation heating, gas phase chemistry, and even the masses of the central stars.

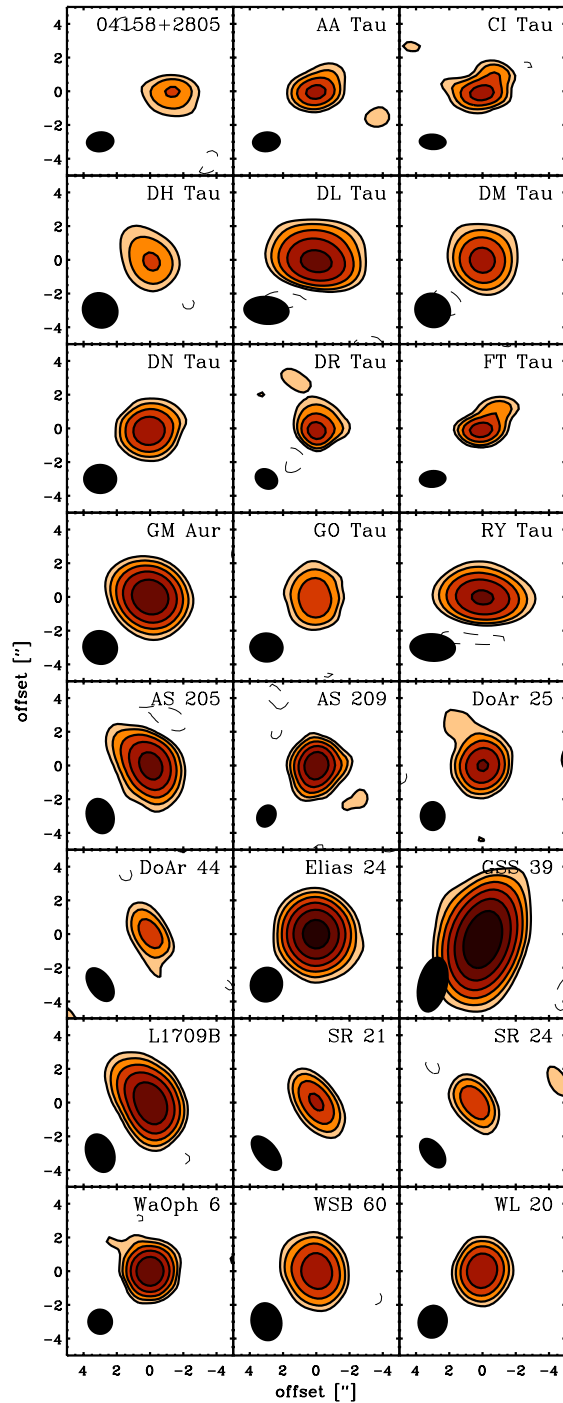


Figure 2.6: Gallery of aperture synthesis SMA continuum images for 24 disks. Each panel is 10 arcsec on a side (~ 1500 AU),

and synthesized beam shapes are shown in the lower left of each panel.

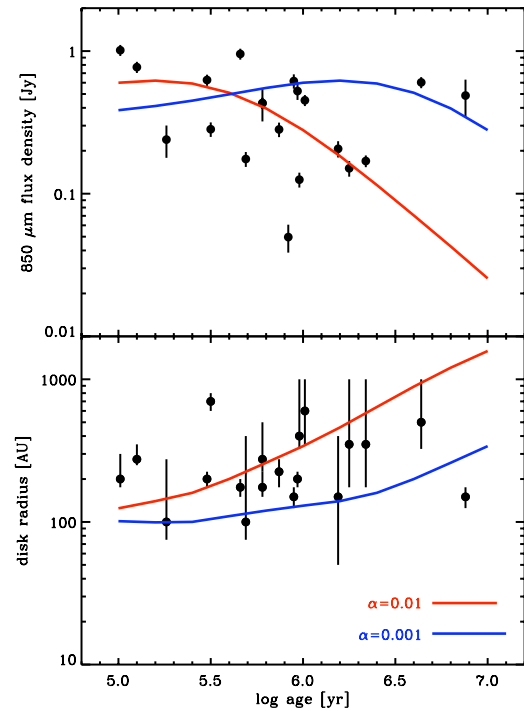


Figure 2.7: The $850 \mu\text{m}$ flux densities (*top*) and best-fit disk radii (*bottom*) as a function of stellar age for the SMA sample. Overlaid are the behaviors of a fiducial accretion disk evolution model [2] with two different turbulent viscosity parameters: $\alpha = 0.01$ (*red*) and $\alpha = 0.001$ (*blue*).

References:

- (1) Andrews, S. M., & Williams, J. P. 2007, ApJ, in press (see astro-ph/0610813)
- (2) Hartmann, L., Calvet, N., Gullbring, E., & D'Alessio, P. 1998, ApJ, 495, 385
- (3) Beckwith, S. V. W., & Sargent, A. I. 1991, ApJ, 381, 250
- (4) Andrews, S. M., & Williams, J. P. 2005, ApJ, 631, 1134
- (5) Draine, B. T. 2006, ApJ, 636, 1114
- (6) Dartois, E., Dutrey, A., & Guilloteau, S. 2003, A&A, 399, 773

Sean M. Andrews (*IfA*)

3 Engineering Highlights

Photonic local oscillator development

Generally speaking, there exists two approaches for the generation of local oscillator power sufficient to operate heterodyne receivers in the submillimeter. One approach is to use an InP Gunn oscillator operating at about 100 GHz, followed by varactor diode frequency multiplier. The other approach uses a YIG (yttrium iron garnet) oscillator operating at about 20 GHz, followed by a cascade of varactor multiplier and amplifier pairs. Unfortunately, the availability of suitable InP devices is limited and amplifier diode frequency multiplier pairs suffer from high cost and large variations of output power across the output bandwidth. An alternate way of generating millimeter-wave radiation is to beat two IR lasers in a photo-mixer. However, previous attempts have failed to produce a local oscillator of sufficient spectral purity and phase stability required to operate an interferometric array. In the receiver lab, we have developed a 200 GHz to 230 GHz local oscillator constructed from mostly commercially available 1550 nm laser communication components. Theoretical and experimental work show that the laser adds negligible phase noise to this photonic local oscillator system and that spectral purity and phase stability are similar to Gunn oscillator based local oscillator output.

The optical path consists of a single 1550 nm diode laser, a lithium niobate optical phase modulator, a Mach Zehnder interferometer (MZI) with a free spectral range of 75 GHz, and a 160 GHz to 260 GHz photomixer whose output is connected to a horn antenna. All of the optical devices and connections are polarization maintaining, and the photomixer was designed and fabricated at the CCLRC Rutherford Appleton Laboratory. The electrical path consists of a YIG synthesizer, operating in the frequency range 14 – 20 GHz, a frequency doubler, and a power amplifier connected to the RF port of the phase modulator. In our scheme, output from the laser is phase modulated at twice the YIG frequency, then converted to an amplitude modulated signal by the MZI. The photomixer, placed at one port of the MZI, generates a frequency comb spaced at twice the modulating frequency. Finally, output from the photomixer passes through a short waveguide section, which cuts off frequencies below 175 GHz, to a pyramidal horn used to couple radiation to the receiver.

The phase of the output radiation from the photonic LO is stabilized using a standard phase-lock system. A lower frequency component of the radio comb, generated by a separate commercial photo-mixer placed at the second output port of the MZI, passes to a harmonic mixer, where it beats with the standard SMA distributed YIG reference signal (6-8 GHz) using a slightly modified SMA digital PLL normally used to lock a Gunn oscillator. The laser frequency is controlled by the laser temperature via a GPIB-based laser con-

troller that is remotely operated by the same server program (tune6) that operates the traditional LOs used on the SMA. In order to produce maximum RF power illuminating the SIS mixer, the frequency of the laser is adjusted to maximize the throughput of the MZI, and final optimization is done with a mechanical tuner on the photomixer block. Aside from the laser controller and amplifier power supply, the photonic LO, shown in Figure 3.1, is packaged into a small size that fits in the space normally allocated to the standard Gunn-multiplier based LO system.

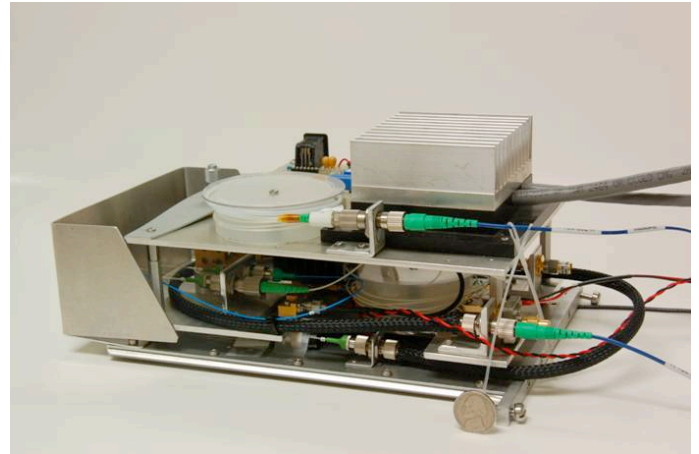


Figure 3.1: Side view of the laser-based millimeter-wave local oscillator

We incorporated the photonic LO into one element (Antenna 6) of a five antenna array for test observations of ^{12}CO $J=2-1$ made towards the ultra-compact HII region G138.295+1.555. Spectra from these observations are plotted in Figure 3.2, both on baselines incorporating Antenna 6 and other baselines of similar lengths. Referring to the Figure, features of comparable width occur on baselines with and without antenna 6, and noise increases with baseline length independent of antenna number. Continuum observations were also made toward the quasar 3c454.3 for a period of about one hour. Figure 3.3 shows the visibility phase as a function of time, again showing an increase in noise for longer baselines, and similar phase stability in time for both photonic and classical LO. In summary, the SMA has proven that the photonic local oscillator operates with adequate phase and frequency stability for radio-interferometry. More widespread use of this technology will be possible as soon as high frequency photo mixers become more readily available and less expensive.

4 Proposal Statistics (November 2006 - April 2007)

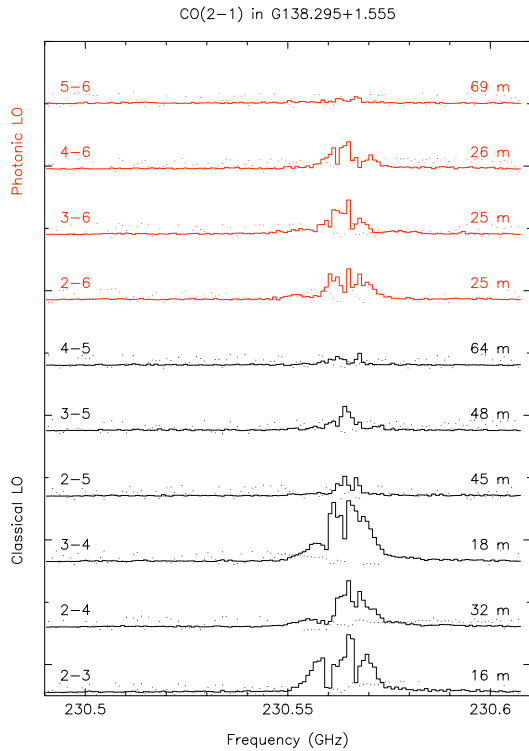


Figure 3.2: Photonic LO test: CO 2-1 line observations

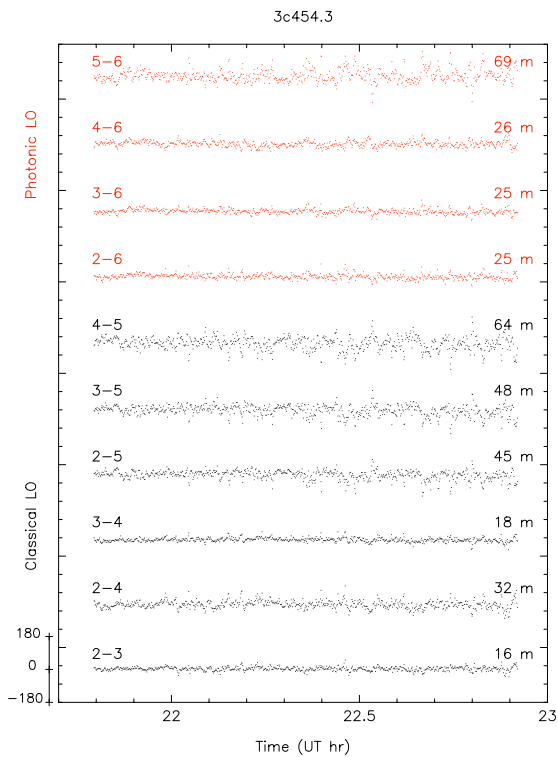


Figure 3.3: Photonic LO test: 3c454.3 continuum visibility phase vs time.

Robert Kimberk, Edward Tong, Todd Hunter,
Robert Christensen, Ray Blundell

The following tables summarize the proposal statistics for semester 2006-09. The proposals are ranked and grouped into three categories: A (best effort to execute), B (may be executed as conditions permit), and C (will not be executed).

Category	CfA P.I.	CfA Co.I.	ASIAA
Star-formation	17	19	15
Extragalactic	17	7	9
Stellar	5	5	2
Planetary	0	0	0
Galactic center	1	1	0
Other	0	1	0
	40	32	26

Frequency band	Tracks allocated	ASIAA
180-250 GHz	10A + 25B	4A + 6B
260-360 GHz	28A + 27B	4A + 4B
620-700 GHz	4A + 0B	0A + 0B
	42A + 52B	8A + 10B

The following is the listing of all SAO and ASIAA A-ranked proposals and the highest ranked UH proposals with the names and affiliations of the principal investigators.

Star Formation

Sean Andrews (*IfA*)

2006-09-H11A

A closer look at a remarkable brown dwarf disk

Tyler Bourke (*CfA*)

2006-09-S053

The Inner Structure of the Protostellar Binary IRAS 16293-2422

Joanna Brown (*Caltech*)

2006-09-S027

High resolution imaging of disks with mid-IR detected gaps

- Paola Caselli (CfA)*
2006-09-S034
Deuterium fractionation in IRAS 05345+3157: where are the massive pre-stellar cores?
- Lincoln Greenhill (CfA)*
2006-09-S025
Submm Water Masers as Tracers of Magnetic Fields in Orion BN/KL
- Naomi Hirano (ASIAA)*
2006-09-A003
SiO J=8-7 and CO J=3-2 from the L1448-mm EHV jet
- Michiel R. Hogerheijde (Leiden Observatory, Leiden, the Netherlands)*
2006-09-S005
Velocity Fields Around the Young Stars TMC1 and L1489 IRS: Infall and Rotation
- Jes K. Jorgensen (CfA)*
2006-09-S047
The Importance of Strong Interstellar Radiation Fields on the Temperature of Protostellar Cores in Orion
- Jes K. Jorgensen (CfA)*
2006-09-S012
Characterizing young disks: SMA observations of Class I young stellar objects
- Yi-Jehng Kuan (NTNU, Taiwan)*
2006-09-A017
Organic Molecules in Class I Protoplanetary Disk
- Ralf Launhardt (MPfA, Heidelberg, Germany)*
2006-09-S028
Disentangling disk and envelope in the CB26 protoplanetary disk system
- Chin-Fei Lee (CfA)*
2006-09-S006
Jet-Disk Systems associated with Low-Mass Protostars
- Silvia Leurini (MPIfR, Bonn, Germany)*
2006-09-S041
IRAS17233: a new hot core in the southern hemisphere
- Rita Mann (IfA)*
2006-09-H023
An SMA survey of the Orion proplyds
- Phil Myers (CfA)*
2006-09-S060
Abundance and Density Structure of the Nearest Cluster-Forming Dense Core
- Nagayoshi Ohashi (ASIAA)*
2006-09-A016
A New Spitzer Source in L1521F: A Candidate for Extremely Young Protostar
- Berengere Parise (MPIfR, Bonn, Germany)*
2006-09-S002
Deuteration in the Orion Bar PDR
- Jenny Patience (Caltech)*
2006-09-S021
Weighing a Very Low Mass Young Object
- Chunhua Qi (CfA)*
2006-09-S039
CO J=6-5 Imaging of Protoplanetary Disks
- Ramprasad Rao (ASIAA)*
2006-09-A026
Mapping the Magnetic Field in NGC 1333 IRAS 4B
- Paula S. Teixeira (CfA)*
2006-09-S063
Measuring the velocity dispersion of a dense protostellar micro-cluster in NGC2264-D-MM1
- Jonathan Williams (IfA)*
2006-09-H024
Structure in the Vega debris disk
- David Wilner (CfA)*
2006-09-S013
Structure in the Vega Debris Disk
- Qizhou Zhang (CfA)*
2006-09-S044
Catching Them Young: Evolution of Youngest Protostellar Outflows
- Extragalactic**
- D.L. Clements (Imperial College, London, UK)*
2006-09-S003

What makes the High Redshift SWIRE Quasar SDSS160705+533558 so luminous in the far-IR?

Len Cowie (IfA)
2006-09-H036
SMA observations of submillimeter selected sources in the HDF-N

Giovanni Fazio (CfA)
2006-09-S037
SMA Imaging Study of the Brightest AzTEC 1100 micron Sources

David H. Hughes (INAOE, Tonantzintla, Puebla, Mexico)
2006-09-S054
Tracing accelerated galaxy formation in a proto-cluster at z 3.8

Jeremy Lim (ASIAA)
2006-09-A002
A Detailed Study of the Molecular Gas Deposited by a X-ray Cooling Flow in Perseus A

Alison Peck (CfA)
2006-09-S001
Very High Resolution Imaging of APM08279

Christine Wilson (McMaster University, Halminton, Ontario)
2006-09-S042
Gas Morphology and Dynamics in Infrared-Luminous Galaxies

Stellar

Valentin Bujarrabal (OAN, Alcala de Henares, Spain)
2006-09-S024
CO J=6-5 and J=3-2 mapping of the rotating disk in IRAS 18059-3211 (Gomez's Hamburger)

Nimesh Patel (CfA)
2006-09-S069
A Submillimeter Wavelength Line Survey of IRC+10216

Galactic Center

James Moran (CfA)
2006-09-S068
Measuring the Spin and Accretion Rate of Sagittarius A*

5 Recent SMA publications

A SLOWLY EXPANDING DISK AND FAST BIPOLAR OUTFLOW FROM THE S STAR π^1 GRUIS

Po-Jian Chiu¹, Chi-Thiem Hoang², Dinh-V-Trung², Jeremy Lim², Sun Kwok², Naomi Hirano², C. Muthu²

(1) National Central University, (2) ASIAA

We study the molecular outflow of the nearby evolved S star π^1 Gru. We imaged the outflow in CO J=2-1 and dust continuum with the Submillimeter Array. The CO emission was detected over a very broad velocity width of ~ 90 km s⁻¹. Our high-resolution images show that the outflow at low velocities (≤ 15 km s⁻¹) is elongated east-west and at high velocities (≥ 25 km s⁻¹) is displaced north (at redshifted velocities) and south (blueshifted velocities) of center as defined by the dust continuum source. We model the spatial-kinematic structure of the low-velocity outflow as a flared disk with a central cavity of radius 200 AU and an expansion velocity of 11 km s⁻¹, inclined by 55° to our line of sight. We attribute the high-velocity component to a bipolar outflow that emerges perpendicular to this disk with a velocity of up to ~ 45 km s⁻¹. This high-velocity outflow may play an important role in shaping the gas envelope previously ejected by the AGB star and thus produce a bipolar morphology when the object evolves into a proto-planetary nebula.

ApJ, 2006, 645, 605

MAGNETIC FIELDS IN THE FORMATION OF SUN-LIKE STARS

J. M. Girart¹, R. Rao², D. P. Marrone³

(1) CSIC-IEEC, (2) ASIAA, (3) CfA

We report high-angular-resolution measurements of polarized dust emission toward the low-mass protostellar system NGC 1333 IRAS 4A. We show that in this system the observed magnetic field morphology is in agreement with the standard theoretical models of the formation of Sun-like stars in magnetized molecular clouds at scales of a few hundred astronomical units; gravity has overcome magnetic support, and the magnetic field traces a clear hour-glass shape. The magnetic field is substantially more important than turbulence in the evolution of the system, and the initial misalignment of the magnetic and spin axes may have been important in the formation of the binary system.

Science, 2006, 313, 812

650 GHz CONTINUUM AND C18O (6-5) OBSERVATIONS OF G240.31+0.07 WITH THE SUBMILLIMETER ARRAY

Huei-Ru Chen^{1,2}, Yu-Nung Su², Sheng-Yuan Liu², Todd R. Hunter³, David J. Wilner³, Qizhou Zhang³, Jeremy Lim², Paul T. P. Ho^{2,3}, Nagayoshi Ohashi², & Naomi Hirano²

(1) National Tsing Hua University, (2) ASIAA, (3) CfA

We report a dual-band observation at 223 and 654 GHz (460 μm) toward an ultracompact (UC) HII region, G240.31+0.07, with the Submillimeter Array. With a beam size of $1.''5 \times 0.''8$, the dust continuum emission is resolved into two clumps, with clump A coincident well with an H₂O maser and the UC HII region. The newly discovered clump B, about $1.''3 (\simeq 8.3 \times 10^3 \text{ AU})$ to the southwest of clump A, is also associated with H₂O masers and may be a more recent star-forming site. The continuum flux densities imply an opacity spectral index of $\beta = 1.5 \pm 0.3$, suggestive of a value lower than the canonical 2.0 found in the interstellar medium and in cold, massive cores. The presence of hot ($\simeq 100 \text{ K}$) molecular gas is derived by the brightness ratio of two H₂CO lines in the 223 GHz band. A radial velocity difference of $2.5 \pm 0.4 \text{ km s}^{-1}$ is found between the two clumps in C¹⁸O (6–5) emission. The total (nebular and stellar) mass of roughly $58M_{\odot}$ in the central region is close to, but not by far larger than, the minimum mass required for the two clumps to be gravitationally bound for binary rotation. Our continuum data do not suggest a large amount of matter associated with the H₂ knots that were previously proposed to arise from a massive disk or envelope.

Accepted for publication in *ApJ* ([astro-ph/00113667](https://arxiv.org/abs/astro-ph/00113667))

SWAS OBSERVATIONS OF WATER VAPOR IN THE VENUS MESOSPHERE

M. A. Gurwell¹, G. J. Melnick¹, V. Tolls¹, E. Bergin², B. M. Patten¹

(1) CfA, (2) Univ. of Michigan

We present the first detections of the ground state ground-state H₂¹⁶O ($1_{10} - 1_{01}$) rotational transition (at 556.9 GHz) and the ¹³CO (5-4) rotational transition from the atmosphere of Venus, measured with the Submillimeter Wave Astronomy Satellite (SWAS). The observed spectral features of these submillimeter transitions originate primarily from the 70–100 km altitude range, within the Venus mesosphere. Observations were obtained in December 2002, and January, March, and July 2004, coarsely sampling one Venus diurnal period as seen from Earth. Complementary observations of the CO(2-1) rotational transition were also obtained with the Submillimeter Array.

The measured water vapor absorption line depth shows large variability among the four observing periods, with strong detections of the line in December 2002 and July 2004, and no detections in January and March 2004. Retrieval of atmospheric parameters was performed using a multi-transition inversion algorithm, combining simultaneous retrievals of temperature, carbon monoxide, and water profiles under imposed constraints. Analysis of the SWAS spectra resulted in measurements or upper limits for the globally averaged mesospheric water vapor abundance

for each of the four observation periods, finding variability over at least two orders of magnitude. The results are consistent with both temporal and diurnal variability, but with short-term fluctuations clearly dominating. These results are fully consistent with the long-term study of mesospheric water vapor from millimeter and submillimeter observations of HDO (Sandor, B.J. and Clancy, R.T., 2005. Water vapor variations in the Venus mesosphere from microwave spectra. *Icarus* 177, 129-143).

The December 2002 observations detected very rapid change in the mesospheric water abundance. Over five days, a deep water absorption feature consistent with a water vapor abundance of 4.5 ± 1.5 parts per million suddenly gave way to a significantly shallower absorption, implying a decrease in the water vapor abundance by a factor of nearly 50 in less than 48 hours. In 2004, similar changes in the water vapor abundance were measured between the March and July SWAS observing periods, but variability on timescales of less than a week was not detected.

The mesospheric water vapor is expected to be in equilibrium with aerosol particles, primarily composed of concentrated sulfuric acid, in the upper haze layers of the Venus atmosphere. If true, moderate amplitude (10-15 K) variability in mesospheric temperature, previously noted in millimeter spectroscopy observations of Venus, can explain the rapid water vapor variability detected by SWAS.

Accepted for publication in *Icarus*, 7 Dec 2006

INVESTIGATING GRAIN GROWTH IN DISKS AROUND SOUTHERN T TAURI STARS AT MILLIMETRE WAVELENGTHS

D. Lommen¹, C. M. Wright², S. T. Maddison³, J. K. Jørgensen⁴, T. L. Bourke⁴, E. F. van Dishoeck¹, A. Hughes³, D. J. Wilner⁴, M. Burton⁵, H. Jan van Langevelde^{1,6}

(1) Leiden Observatory, (2) School of Physical, Environmental and Mathematical Sciences, Canberra, (3) Center for Astrophysics and Supercomputing, Hawthorn, (4) CfA, (5) School of Physics, Sydney, (6) Joint Institute for VLBI in Europe, Dwingeloo

CONTEXT - Low-mass stars form with disks in which the coagulation of grains may eventually lead to the formation of planets. It is not known when and where grain growth occurs, as models that explain the observations are often degenerate. A way to break this degeneracy is to resolve the sources under study. AIMS - To find evidence for the existence of grains of millimetre sizes in disks around in T Tauri stars, implying grain growth. METHODS - The Australia Telescope Compact Array (ATCA) was used to observe 15 southern T Tauri stars, five in the constellation Lupus and ten in Chamaeleon, at 3.3 millimetre. The five Lupus sources were also observed with the Submillimeter Array (SMA) at 1.4 mm. Our new data are complemented with data from the literature to determine the slopes of the spectral energy distributions in the millimetre regime.

RESULTS - Ten sources were detected at better than 3σ with the ATCA, with $\sigma \sim 1\text{--}2$ mJy, and all sources that were observed with the SMA were detected at better than 15σ , with $\sigma \sim 4$ mJy. Six of the sources in our sample are resolved to physical radii of ~ 100 AU. Assuming that the emission from such large disks is predominantly optically thin, the millimetre slope can be related directly to the opacity index. For the other sources, the opacity indices are lower limits. Four out of six resolved sources have opacity indices $\lesssim 1$, indicating grain growth to millimetre sizes and larger. The masses of the disks range from < 0.01 to $0.08 M_{\odot}$, which is comparable to the minimum mass solar nebula. A tentative correlation is found between the millimetre slope and the strength and shape of the $10 \mu\text{m}$ silicate feature, indicating that grain growth occurs on similar (short) timescales in both the inner and outer disk.

Accepted for publication in A&A (astro-ph/0610667)

AN UNAMBIGUOUS DETECTION OF FARADAY ROTATION IN SAGITTARIUS A*

D. P. Marrone¹, J. M. Moran¹, J.-H. Zhao¹, R. Rao²

(1) CfA, (2) ASIAA

The millimeter/submillimeter wavelength polarization of Sgr A* is known to be variable in both magnitude and position angle on time scales down to a few hours. The unstable polarization has prevented measurements made at different frequencies and different epochs from yielding convincing measurements of Faraday rotation in this source. Here we present observations made with the Submillimeter Array polarimeter at 227 and 343 GHz with sufficient sensitivity to determine the rotation measure at each band without comparing position angles measured at separate epochs. We find the 10-epoch mean rotation measure to be $(-5.6 \pm 0.7) \times 10^5 \text{ rad m}^{-2}$; the measurements are consistent with a constant value. We conservatively assign a 3σ upper limit of $2 \times 10^5 \text{ rad m}^{-2}$ to rotation measure changes, which limits accretion rate fluctuations to 25%. This rotation measure detection limits the accretion rate to less than $2 \times 10^{-7} M_{\odot} \text{ yr}^{-1}$ if the magnetic field is near equipartition, ordered, and largely radial, while a lower limit of $2 \times 10^{-9} M_{\odot} \text{ yr}^{-1}$ holds even for a sub-equipartition, disordered, or toroidal field. The mean intrinsic position angle is $167 \pm 7^{\circ}$ and we detect variations of $31(+18/-9)^{\circ}$. These variations must originate in the submillimeter photosphere, rather than arising from rotation measure changes.

Accepted for publication in ApJL (astro-ph/0611791)

THE MOLECULAR ENVELOPE AROUND THE RED SUPERGIANT VY CMA

S. Muller, D. V-Trung, J. Lim, N. Hirano, C. Muthu, S. Kwok
ASIAA

We present millimeter interferometric observations of the

molecular envelope around the red supergiant VY CMA with the Submillimeter Array (SMA). The high angular resolution ($< 2''$) allows us to derive the structure of the envelope as observed in the 1.3 mm continuum, 12CO(2-1), 13CO(2-1) and SO(6,5-5,4) lines emission. The circumstellar envelope is resolved into three components: a dense, compact and dusty central component, embedded in a more diffuse and extended envelope plus a high velocity component. We construct a simple model, consisting of a spherically symmetric slowly expanding envelope and bipolar outflows with a wide opening angle ($\sim 120^{\circ}$) viewed close to the line of sight ($i = 15^{\circ}$). Our model can explain the main features of the SMA data and previous single-dish CO multi-line observations. An episode of enhanced mass loss along the bipolar direction is inferred from our modeling. The SMA data provide a better understanding of the complicated morphology seen in the optical/IR high resolution observations.

Accepted for publication in ApJ (astro-ph/0611547)

A MASSIVE BIPOLAR OUTFLOW AND A DUSTY TORUS WITH LARGE GRAINS IN THE PRE-PLANETARY NEBULA IRAS 22036+5306

R. Sahai¹, K. Young², N.A. Patel², C. S'anchez Contreras¹, M. Morris³

(1) JPL, Caltech, (2) CfA, (3) UCLA

We report high angular-resolution ($\sim 1''$) CO J=3-2 interferometric mapping, using the Submillimeter Array (SMA), of IRAS 22036+5306 (I22036), a bipolar pre-planetary nebula (PPN) with knotty jets discovered in our HST Snapshot survey of young PPNs. In addition, we have obtained supporting lower-resolution ($\sim 10''$) CO and ^{13}CO J=1-0 observations with the Owens Valley Radio Observatory (OVRO) interferometer, as well as optical long-slit echelle spectra at the Palomar Observatory. The CO J=3-2 observations show the presence of a very fast ($\sim 220 \text{ km s}^{-1}$), highly collimated, massive ($0.03 M_{\odot}$) bipolar outflow with a very large scalar momentum (about $10^{39} \text{ g cm s}^{-1}$), and the characteristic spatio-kinematic structure of bow-shocks at the tips of this outflow. The H α line shows an absorption feature blue-shifted from the systemic velocity by $\sim 100 \text{ km s}^{-1}$, which most likely arises in neutral interface material between the fast outflow and the dense walls of the bipolar lobes at low latitudes. Since the expansion age of the outflow as determined from our data is only about 25 years, much smaller than the time required by radiation pressure to accelerate the observed bipolar outflow to its current speed ($\gtrsim 10^5 \text{ yr}$), the fast outflow in I22036, as in most PPNs, cannot be driven by radiation pressure. The total molecular mass ($0.065 M_{\odot}$) is much less than that derived from a previous detailed model of the near to far-infrared SED of this object (showing the presence of a large, cool dust shell of total mass $4.7 M_{\odot}$), most likely due to the interferometric observa-

tions resolving out the CO flux from the dust shell due to its size. We find an unresolved source of submillimeter (and millimeter-wave) continuum emission in I22036, implying a very substantial mass (0.02-0.04 M_{\odot}) of large (radius $\gtrsim 1$ mm), cold ($\lesssim 50$ K) dust grains associated with I22036's toroidal waist. We also find that the $^{13}\text{C}/^{12}\text{C}$ ratio in I22036 is very high (0.16), close to the maximum value achieved in equilibrium CNO-nucleosynthesis (0.33). The combination of the high circumstellar mass (i.e., in the extended dust shell and the torus) and the high $^{13}\text{C}/^{12}\text{C}$ ratio in I22036 provides strong support for this object having evolved from a massive ($\gtrsim 4 M_{\odot}$) progenitor in which hot-bottom-burning has occurred.

Accepted for publication in ApJ (astro-ph/0609455)

DETECTION OF CO HOTSPOTS ASSOCIATED WITH YOUNG CLUSTERS IN THE SOUTHERN STARBURST GALAXY NGC 1365

K. Sakamoto^{1,2}, P. T. P. Ho^{1,3}, R.-Q. Mao⁴, S. Matsushita³, A. B. Peck¹

(1) CfA, (2) NAOJ, (3) ASIAA, (4) Purple Mount Observatory

We have used the Submillimeter Array for the first interferometric CO imaging toward the starburst-Seyfert nucleus of the southern barred spiral galaxy NGC 1365, which is one of the four galaxies within 30 Mpc that have $L_{8-1000\mu\text{m}} \geq 10^{11} L_{\odot}$. Our mosaic maps of ^{12}CO , ^{13}CO , and C^{18}O (J=2-1) emission at up to 2'' (200 pc) resolutions have revealed a circumnuclear gas ring and several CO clumps in the central 3 kpc. The molecular ring shows morphological and kinematical signs of bar-driven gas dynamics, and the region as a whole is found to follow the star formation laws of Kennicutt. We have found that some of the gas clumps and peaks in CO brightness temperature, which we collectively call CO hotspots, coincide with the radio and mid-infrared sources previously identified as dust-enshrouded super star clusters. This hotspot-cluster association suggests that either the formation of the most massive clusters took place in large molecular gas concentrations (of $\Sigma_{\text{mol}} \sim 10^3 M_{\odot} \text{pc}^{-2}$ in 200 pc scales) or the clusters have heated their ambient gas to cause or enhance the CO hotspots. The active nucleus is in the region of weak CO emission and is not associated with distinctive molecular gas properties.

Accepted for publication in ApJ (astro-ph/0609805)

STRUCTURE AND KINEMATICS OF CO (J=2-1) EMISSION IN THE CENTRAL REGION OF NGC 4258

S. Sawada-Satoh¹, P. T. P. Ho^{1,2}, S. Muller¹, S. Matsushita¹, J. Lim¹

(1) ASIAA, (2) CfA

We present ^{12}CO (J=2-1) observations towards the central

region of the Seyfert 2 galaxy NGC 4258 with the Submillimeter Array (SMA). Our interferometric maps show two arm-like elongated components along the major axis of the galaxy, with no strong nuclear concentration. The CO (2-1) morphology and kinematics are similar to previous CO (1-0) results. The velocity field of the components agrees with the general galactic rotation, except for the east elongated component, which shows a significant velocity gradient along the east-west direction. In order to account for the velocity field, we propose the kinematical model where the warped rotating disk is also expanding. The line ratio of CO(2-1)/CO(1-0) reveals that the eastern component with the anomalous velocity gradient appears to be warmer and denser. This is consistent with the gas in this component being closer to the center, being heated by the central activities, and possibly interacted by expanding motions from the nuclear region.

Accepted for publication in ApJ (astro-ph/0612303)

MOLECULAR CO OUTFLOWS IN THE L1641-N CLUSTER: KNEADING A CLOUD CORE

T. Stanke^{1,2,3} & J. P. Williams³

(1) ESO, Garching (2) MPIfR, Bonn, (3) IfA

We present results of 1.3 mm interferometric and single-dish observations of the center of the L1641-N cluster in Orion. Single-dish wide-field continuum and CO (2-1) observations reveal the presence of several molecular outflows driven by deeply embedded protostellar sources. At higher angular resolution, the dominant millimeter source in the cluster center is resolved into a pair of protostars (L1641-N-MM1 and MM3), each driving a collimated outflow, and a more extended, clumpy core. Low-velocity CO line-wing emission is widely spread over much of the cluster area. We detect and map the distribution of several other molecular transitions (^{13}CO , C^{18}O , ^{13}CS , SO, CH_3OH , CH_3CN , and OCS). CH_3CN and OCS may indicate the presence of a hot corino around L1641-N-MM1. We tentatively identify a velocity gradient over L1641-N-MM1 in CH_3CN and OCS, oriented roughly perpendicular to the outflow direction, perhaps indicative of a circumstellar disk. An analysis of the energy and momentum load of the CO outflows, along with the notion that apparently a large volume fraction is affected by the multiple outflow activity, suggests that outflows from a population of low-mass stars might have a significant impact on clustered (and potentially high-mass) star formation.

Accepted for publication in AJ (astro-ph/0611052)

SILICON MONOXIDE OBSERVATIONS REVEAL A CLUSTER OF HIDDEN COMPACT OUTFLOWS IN THE OMC1 SOUTH REGION

L. A. Zapata^{1,2}, P. T. P. Ho^{2,3}, L. F. Rodriguez¹, C. R. O'Dell⁴, Q. Zhang², A. Muench²

(1) CRyA, UNAM, (2) CfA, (3) ASIAA, (4) Vanderbilt Univ.

We present high angular resolution ($2''.8 \times 1''.7$) SiO $J=5 \rightarrow 4$; $v = 0$ line observations of the OMC1S region in the Orion Nebula made using the Submillimeter Array (SMA). We detect for the first time a cluster of four compact bipolar and monopolar outflows that show high, moderate and low velocity gas and appear to be energized by millimeter and infrared sources associated with this region. The SiO molecular outflows are compact (<3500 AU), and in most of the cases, they are located very close to their exciting sources. We thus propose that the SiO thermal emission is tracing the youngest and most highly excited parts of the outflows which cannot be detected by other molecules. Moreover, since the ambient cloud is weak in the SiO line emission, these observations can reveal flows that in other molecular transitions will be confused with the ambient velocity cloud emission. Analysis of their positional-velocity diagrams show that some components of these outflows may be driven by wide-angle winds very close to the exciting object. Finally, we find that some of these SiO outflows seem to be the base of powerful Herbig-Haro jets and large-scale molecular flows that emanate from a few arcseconds around this zone. In particular, we find a strongly excited SiO bipolar outflow with a P.A. of $\sim 100^\circ$, that is likely energized by the luminous ($\sim 3 \times 10^3 L_\odot$) infrared protostar "B" and could be the base of the remarkable object HH269.

Accepted to ApJ ([astro-ph/0608133](http://arxiv.org/abs/astro-ph/0608133))

MULTIPLE JETS FROM THE HIGH-MASS (PROTO)STELLAR CLUSTER AFGL5142

Q. Zhang¹, T. R. Hunter¹, H. Beuther², T. K. Sridharan¹, S.-Y. Liu³, Y.-N. Su³, H.-R. Chen³, Y. Chen³

(1) CfA, (2) MPIfA, Heidelberg, (3) ASIAA

We present studies of a massive protocluster AFGL5142 in the $J=2-1$ transition of the CO isotopologues, SO, CH₃OH and CH₃CN lines, as well as continuum at 225 GHz and 8.4 GHz. The 225 GHz continuum emission reveals three prominent peaks MM-1, MM-2 and MM-3. MM-1 and MM-2 are associated with strong CH₃CN emission with temperatures of 90 ± 20 and 250 ± 40 K, respectively, while both MM-1 and MM-3 are associated with faint continuum emission at 8.4 GHz. Additional dust continuum peaks MM-4 and MM-5 appear to be associated with H₂O masers. With many continuum sources at cm and mm wavelengths, and those already identified in the infrared, this region is forming a cluster of stars. The CO and SO emission reveals at least three molecular outflows originating from the center of the dust core. The outflows are well collimated, with terminal velocities up to 50 km s^{-1} from the cloud velocity. Outflow A coincides with the SiO jet identified previously by Hunter et al. (1999). Since jet-like outflows and disk-mediated accretion process are physically connected, the well collimated outflows indicate that even in this cluster environment, accretion is responsible for the formation of individual stars in the cluster.

Accepted for publication in ApJ ([astro-ph/0612027](http://arxiv.org/abs/astro-ph/0612027))

6 Other news

Call for proposals

A call for proposals for the 1 May – 31 October 2007 period will be issued in January 2007. The anticipated deadline will be 1 March 2007. Please watch the SMA website <http://sma-www.harvard.edu> for the announcement.



A panoramic view of the Mauna Kea observatories. The SMA is in compact configuration. Photograph by Paul Yamaguchi.

The SMA newsletter is edited by Nimesh Patel (npatel@cfa.harvard.edu). This issue includes contributions from Sean Andrews, Ray Blundell, Mark Gurwell, Jim Moran, David Wilner, and Qizhou Zhang.

Submillimeter Array

Harvard-Smithsonian Center for Astrophysics
60 Garden Street, MS 78, Cambridge, MA 02138, USA

<http://sma-www.harvard.edu>

<http://sma1.sma.hawaii.edu>

SMA Hilo office

645 North A'ohoku Place

Hilo, Hawaii 96720

Phone:(808) 961-2920

Fax:(808) 961-2921

Academia Sinica Institute of Astronomy & Astrophysics

P. O. Box 23-141, Taipei 10617, Taiwan R. O. C.

<http://www.asiaa.sinica.edu.tw/>